Whitening in Range to Improve Weather Radar Spectral Moment Estimates. Part I: Formulation and Simulation

SEBASTIÁN M. TORRES

Cooperative Institute for Mesoscale Meteorological Studies, University of Oklahoma, and National Severe Storms Laboratory, Norman, Oklahoma

DUŠAN S. ZRNIĆ

National Severe Storms Laboratory, Norman, Oklahoma

(Manuscript received 29 May 2002, in final form 14 March 2003)

ABSTRACT

A method for estimation of spectral moments on pulsed weather radars is presented. This scheme operates on oversampled echoes in range; that is, samples of in-phase and quadrature-phase components are collected at a rate several times larger than the reciprocal of the transmitted pulse length. The spectral moments are estimated by suitably combining weighted averages of these oversampled signals in range with usual processing of samples (spaced at the pulse repetition time) at a fixed range location. The weights in range are derived from a whitening transformation; hence, the oversampled signals become uncorrelated and, consequently, the variance of the estimates decreases significantly. Because the estimate errors are inversely proportional to the volume scanning times, it follows that storms can be surveyed much faster than is possible with current processing methods, or equivalently, for the current volume scanning time, accuracy of the estimates can be greatly improved. This significant improvement is achievable at large signal-to-noise ratios.

1. Introduction

Doppler weather surveillance radars probe the atmosphere and retrieve spectral moments for each resolution volume in the surrounding space. In computing these moments, it is customary to average signals from many pulses to reduce the statistical uncertainty of the estimates. With such processing, the variance reduction of averaged estimates is inversely proportional to the equivalent number of independent samples, which depends on the correlation between samples ρ and the total number of averaged samples (or pulses) M (Walker et al. 1980). The number of samples available for averaging is determined by the pulse repetition time T_s and the dwell time, which is usually controlled by the required azimuthal resolution. If averaging along sample time is not enough to keep estimation errors below acceptable limits, it is possible to trade range resolution for estimate accuracy by averaging a few samples along range time. From an operational point of view, we are faced with conflicting requirements. On the one hand, large estimation errors restrict the applicability of weather surveillance radars for precise quantification and identification of weather phenomena. On the other hand, the need for faster updates between volume scans calls for faster antenna rotation rates, which limit the number of samples available for each resolution volume. As mentioned before, the number of samples is inversely related to the variance of estimates.

Several solutions have been proposed to reduce spectral moment errors in weather surveillance radars. In the quest for finding better estimators of spectral moments, Zrnić (1979) showed that maximum likelihood (ML) estimators yield errors one order of magnitude less than those obtained with conventional autocovariance methods. Later, Frehlich (1993) improved Zrnić's results and derived simplified expressions to test new estimators based on the ML approach. Due to the complexity of ML estimators, researchers focused on ways to simplify spectral moment estimators by assuming knowledge of some of the underlying parameters of the weather signal. Bamler (1991) computed the Cramer–Rao lower bound (CRLB) for Doppler frequency estimates assuming both the correlation (or spectrum) of samples and signal-to-noise ratio (SNR) are known. Later, Chornoboy (1993) obtained an optimal estimator for Doppler velocity that is simpler than ML formulations, but again, the SNR and the spectrum width were assumed to be known. Summarizing, ML estimators provide better accuracy compared with classic estimators (Zrnić 1979) and are

Corresponding author address: Dr. Sebastián M. Torres, NSSL, 1313 Halley Circle, Norman, OK 73069.
E-mail: sebastian.torres@noaa.gov

© 2003 American Meteorological Society

only moderately complex if the spectrum width is known a priori. However, this last assumption restricts their applicability because the correlation coefficient of the weather echo along sample time is not known and must be estimated. That is, to estimate spectral moments, the joint distribution of signal power, mean Doppler velocity, and spectrum width would need to be calculated, which turns out to be computationally very intensive. Dias and Leitão (2000) proposed ML estimators that do not exhibit the characteristic computational burden. They derived a nonparametric method to obtain ML estimates of spectral moments from weighted sums of autocovariance estimates; the only assumption is that the power spectral density of the underlying process is bandlimited.

Schulz and Kostinski (1997) suggested that knowledge of the correlation coefficient of weather-echo time series could improve the variance of spectral moment estimates. By means of the whitening transformation (i.e., a linear operation that decorrelates echo samples), they devised estimators that theoretically achieve the CRLB. Further, Koivunen and Kostinski (1999) explored practical aspects of the whitening transformation on estimation of signal power. A principal obstacle to the application of the whitening transformation on the time series is the need to know (or estimate) the correlation coefficient of the signal. These authors suggest ways to overcome this difficulty and call for an experimental study to verify the technique. Using the whitening approach, Frehlich (1999) investigated the performance of ML estimators of spectral moments under the assumption of a known spectrum width. Although Frehlich concluded that the estimator derived by Schultz and Kostinski cannot be applied to the case of finite SNR, Kostinski and Koivunen (2000) showed that the problem is not in the estimator but in the Gaussian assumption for the Doppler spectrum. In their work, they suggested simple numerical recipes intended to avoid the so-called Gaussian anomaly.

Range oversampling to improve the estimates of periodograms was explored by Urkowitz and Katz (1996). They acknowledged that the periodograms for each range location are correlated; they computed the equivalent number of uncorrelated range samples and showed that the variance reduction is not optimal. Strauch and Frehlich (1998) considered oversampled signals in range to estimate Doppler velocity within one pulse. This approach fails because the phase shift within a pulse is smaller than the uncertainty of the estimates; the authors point out that simple averaging is not enough to achieve the required equivalent number of independent samples. Acquisition and processing of samples over finer range scales was investigated also in the context of pulse compression. Pulse compression can be applied to increase the equivalent number of independent samples by averaging high-resolution estimates in range (Mudukutore et al. 1998). However, most ground-based weather surveillance radars do not use pulse compression due to the required larger transmission bandwidths.

Range oversampling and whitening can be used to increase the equivalent number of independent samples without increasing the transmission bandwidth. The main advantage of this technique is that the whitening transformation is derived from a known correlation function. In a rather short but important study, Dias and Leitão (1993) derived an iterative technique to obtain ML estimates of spectral moments. They consider both the time and space variables and assume a known correlation in range. Implicit in their solution is whitening of the signals in range; thus, it is likely the earliest application of this technique to radar remote sensing. More recently, Fjørtoft and Lopès (2001) proposed a method for estimating the reflectivity in synthetic aperture radar (SAR) images with correlated samples (pixels). The method is based on a modified whitening transformation that exhibits low computational complexity and is suitable for oversampled data.

This paper describes an application of the whitening transformation in range that increases the equivalent number of independent samples while keeping the dwell time constant with no significant degradation of the range resolution. Obtaining more independent samples reduces the estimate errors at the same antenna rotation rate or speeds up volume scans while keeping the errors at previous levels. Our work has been inspired by Schulz and Kostinski (1997) but shares some common elements with the work of Dias and Leitão (1993). In simulation studies we consider a receiver with a large bandwidth and a perfect rectangular pulse. We use autocovariance processing in sample time and examine in detail the effects of white noise. At the end we briefly describe some other practical aspects and trade-offs.

2. Why whitening?

Current implementations of spectral moment estimators use a simple method of averaging samples in range at the expense of degradation in range resolution. Simple averaging, however, does not yield the best performance when the observations are correlated. Schulz and Kostinski (1997) computed the variance bounds for reflectivity estimates and demonstrated that they do not depend on the correlation structure of the observations. Hence, it can be inferred that it is not the correlation between observations that limits the accuracy of a given estimator but the way those observations are used to compute the estimates. Therefore, it is reasonable to think that knowledge of the correlation coefficient $\rho(mT_s)$ could be used to formulate estimators that attain the CRLB. In their work, Schulz and Kostinski proposed whitening the time series data along sample time to produce uncorrelated samples. The main drawback for this technique is that the whitening transformation depends on other meteorological parameters such as the spectrum width. Dias and Leitão (1993) derived man-

ageable approximate solutions to the ML estimators of spectral moments for signals that are oversampled in range. Their solution, although not immediately transparent to readers, amounts to whitening the samples in range and applying Fourier transforms for estimating spectral moments.

We suggest combining the whitening transformation of samples in range with autocovariance processing in sample time and thus improving the spectral moment estimates. The proposed processing increases the equivalent number of independent samples in a simple manner while the sacrifice in range resolution is minimal and the transmission bandwidth is not broadened. While the correlation of samples separated by T_s needs to be estimated for each particular case (it depends on the meteorological conditions being observed), samples spaced in range exhibit a correlation coefficient that can be exactly computed a priori; the underlying assumption here is that the mean echo power changes very little over the averaging interval in range. We elaborate more on this fundamental constraint later. By exactly knowing the correlation coefficient, it is possible to apply the whitening transformation without worrying about the pitfalls originating from an estimated quantity. As a result, the equivalent number of independent samples becomes equal to the number of available samples, and the variance reduction through averaging is maximized. Maximization of the equivalent number of independent samples leads to the following.

- For the same uncertainty as that obtained with correlated samples, faster scan rates are possible, as the total number of samples M for a resolution volume is determined by the pulse repetition time and the dwell time. Rapid acquisition of volumetric radar data has significant scientific and practical ramifications. For example, observations at minute intervals are required to understand the details of vortex formation and demise near the ground. Even faster rates of volumetric data are required to determine the presence of transverse winds. Fast update rates would also yield more timely warnings of impending severe weather phenomena such as tornadoes and strong winds.
- For the same scanning rates, lower uncertainties can be obtained, making the use of polarimetric variables feasible for accurate rainfall estimation and hydrometeor identification.

With the advent of digital receivers (Brunkow 1999), oversampling is indeed feasible (Ivić 2001). Therefore, it is possible to maintain the same current radar capabilities (as with a digital matched filter in classical processing) while adding, in parallel, a set of more reliable estimates obtained from whitened oversampled range data.

3. The whitening transformation

The procedure (as depicted in Fig. 1) begins with oversampling in range so that there are L samples during the pulse duration τ (i.e., oversampling by a factor of L). Assume that a range of depth $c\tau$ (where c is the speed of light) is uniformly filled with scatterers, which is a common occurrence for relatively short pulses. For convenience, the contribution from the resolution volume to the received sampled complex voltage $V(nT_s) = I(nT_s) + jQ(nT_s)$ at a fixed time delay nT_s can be decomposed into subcontributions $s(l\tau_o, nT_s)$ from L contiguous elemental shells or ''slabs,'' each $c\tau/2L$ thick. Each of these is an equivalent scattering center. For simplicity τ_o and T_s are dropped hereafter so the indices l and n indicate range-time increments τ_o (sampling time) and sample-time increments T_s (pulse repetition time), respectively. The voltages $s(l, n)$ are identically distributed, complex, Gaussian random variables, where the real and imaginary parts have variances σ^2, and the average power of $s(l, n)$ is $\sigma_s^2 = 2\sigma^2$. A pulse with an arbitrary envelope shape $p(l)$ induces weighting to the contributions from contiguous slabs such that the composite voltage after synchronous detection is

$$V(l, n) = I(l, n) + jQ(l, n) = \left[\sum_{i=0}^{L-1} s(l + i, n)p(L - 1 - i)\right] \star h(l), \quad (1)$$

where the $\star$ denotes convolution and $h(l)$ is the impulse response of the receiver filter. The summation in (1) is

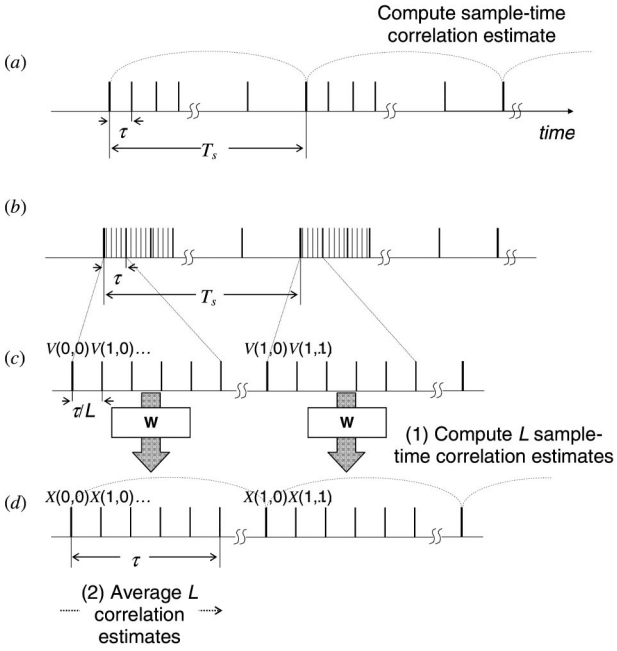

FIG. 1. Depiction of sampling/oversampling in range and processing of the signals. (a) Samples in range with spacing equal to the pulse length τ; standard processing to obtain correlation estimates is indicated; (b) oversampling in range; (c) zoomed presentation of oversampled range locations where range samples to be whitened with matrix **W** are indicated; (d) processing of whitened samples to obtain estimates of correlations in range and average of these estimates in range to reduce the statistical errors.

a correct representation for the composite voltage $V(l, n)$ given that we consider ''scattering centers,'' and each of these implicitly admits integration. Then, as a generalization of (4.40) in Doviak and Zrnić (1993), the correlation of range samples is

$$R_V^{(R)}(l) = \sigma_s^2[p_m(l) \star p_m^*(-l)], \tag{2}$$

where the modified pulse envelope p_m is given by $p_m(l) = p(l) \star h(l)$. Hence, the correlation coefficient of range samples $\rho_V^{(R)}$ is

$$\rho_V^{(R)}(l) = \frac{R_V^{(R)}(l)}{R_V^{(R)}(0)} = \frac{p_m(l) \star p_m^*(-l)}{\sum_{l'=0}^{L-1} p_m^2(l')}. \tag{3}$$

In practice, $\rho_V^{(R)}$ can be evaluated by attenuating the transmitted pulse, injecting it directly into the receiver, and oversampling the result to obtain the modified pulse envelope p_m. Introducing p_m into (3) produces $\rho_V^{(R)}$; this needs to be done only once for a given pulse shape and receiver bandwidth.

The procedure for implementing the whitening transformation follows Koivunen and Kostinski (1999) and is listed here for completeness (and reader convenience). Define the Toeplitz–Hermitian normalized correlation matrix $\mathbf{C}_V^{(R)}$ as

$$\mathbf{C}_V^{(R)} = \begin{bmatrix} 1 & \rho_V^{(R)}(1) & \cdots & \rho_V^{(R)}(L-1) \\ \rho_V^{(R)}(1)^* & 1 & \cdots & \rho_V^{(R)}(L-2) \\ \vdots & \vdots & \ddots & \vdots \\ \rho_V^{(R)}(L-1)^* & \rho_V^{(R)}(L-2)^* & \cdots & 1 \end{bmatrix}. \tag{4}$$

Because this matrix is positive semidefinite (Therrien 1992), it can be decomposed as

$$\mathbf{C}_V^{(R)} = \mathbf{H}^*\mathbf{H}^{\mathrm{T}}, \tag{5}$$

where the superscript T indicates matrix transpose and * is the usual complex conjugation operation. Any $\mathbf{H}$ that satisfies (5) is called a square root of $\mathbf{C}_V^{(R)}$ (Faddeev and Faddeeva 1963) and is the inverse of a whitening transformation matrix,

$$\mathbf{W} = \mathbf{H}^{-1}, \tag{6}$$

which, if applied to the range samples, produces L uncorrelated random variables with identical power (Kay 1993).

In general, the decomposition of the correlation matrix is not unique and many well-known methods can be applied to generate different whitening transformations. Two such methods are the eigenvalue decomposition (Therrien 1992) and Cholesky decomposition, which is equivalent to Gram–Schmidt orthogonalization (Therrien 1992; Papoulis 1984). In the eigenvalue decomposition method, $\mathbf{C}_V^{(R)}$ is represented as $\mathbf{C}_V^{(R)} = \mathbf{U}\mathbf{\Lambda}\mathbf{U}^{*\mathrm{T}}$, where $\mathbf{\Lambda}$ is a diagonal matrix of eigenvalues of $\mathbf{C}_V^{(R)}$, and $\mathbf{U}$ is the unitary matrix whose columns are the eigenvectors of $\mathbf{C}_V^{(R)}$. With this decomposition, an expression of the same form as (5) can be obtained as $\mathbf{C}_V^{(R)} = \mathbf{H}^*\mathbf{H}^{\mathrm{T}} = (\mathbf{U}^*\mathbf{\Lambda}^{1/2})^*(\mathbf{U}^*\mathbf{\Lambda}^{1/2})^{\mathrm{T}}$, where $\mathbf{\Lambda}^{1/2}$ is a diagonal matrix with the square roots of the eigenvalues on the diagonal. With this decomposition, $\mathbf{H} = \mathbf{U}^*\mathbf{\Lambda}^{1/2}$, and $\mathbf{W}$ is obtained as $\mathbf{W} = \mathbf{H}^{-1} = \mathbf{\Lambda}^{-1/2}\mathbf{U}^{\mathrm{T}}$, which is the Mahalanobis transformation (Tong 1995). In the case of Cholesky (or triangular) decomposition, the correlation matrix is factored as $\mathbf{C}_V^{(R)} = \mathbf{T}\mathbf{T}^{*\mathrm{T}}$, where the matrix $\mathbf{T}$ is a lower triangular matrix. Here, $\mathbf{C}_V^{(R)} = \mathbf{H}^*\mathbf{H}^{\mathrm{T}} = (\mathbf{T}^*)^*(\mathbf{T}^*)^{\mathrm{T}}$, and $\mathbf{H} = \mathbf{T}^*$; hence, the whitening matrix $\mathbf{W} = \mathbf{H}^{-1} = (\mathbf{T}^*)^{-1}$ is also lower triangular. A possible advantage of lower triangular $\mathbf{W}$ matrices is that whitening can proceed in a pipeline manner; that is, computations can start as soon as the first sample is taken and progress through subsequent samples. Non-lower-triangular $\mathbf{W}$ matrices require the presence of all data before a whitened sample can be computed.

In the following sections, we denote with $X(l, n)$ the sequence of whitened samples obtained from $V(l, n)$ for a fixed sample time nT_s as

$$X(l, n) = \sum_{j=0}^{L-1} w_{l,j} V(j, n); \qquad l = 0, 1, \ldots, L-1, \tag{7}$$

where $w_{l,j}$ are the entries of the whitening matrix. Alternatively, the previous equation can be written using matrix notation as

$$\mathbf{X}_n = \mathbf{W}\mathbf{V}_n, \tag{8}$$

where $\mathbf{V}_n = [V(0, n), V(1, n), \ldots, V(L-1, n)]^{\mathrm{T}}$ and $\mathbf{X}_n = [X(0, n), X(1, n), \ldots, X(L-1, n)]^{\mathrm{T}}$. It is important to note that regardless of the method used to decompose $\mathbf{C}_V^{(R)}$, the whitening procedure is given by (8), and even though the whitening matrices may be different, the results in terms of data decorrelation are statistically equivalent.

4. The noise enhancement effect

The presence of noise is inherent in every radar system; therefore, it is necessary to analyze the performance of the whitening transformation, under noisy conditions. Let $V = V_S + V_N$, where the subscripts S and N stand for signal and noise components, respectively. When applying the whitening transformation, both signal and noise are similarly affected:

$$\mathbf{X} = \mathbf{W}\mathbf{V} = \mathbf{W}\mathbf{V}_S + \mathbf{W}\mathbf{V}_N = \mathbf{X}_S + \mathbf{X}_N. \tag{9}$$

For simplicity, we dropped the subscript ''n'' that is used to indicate sample time. From (9), we can see that the signal is whitened and the noise, which was white prior to the whitening transformation, becomes colored.

Let us apply the transformation matrix to the data (8) and compute the range-time correlation $\mathbf{R}_X^{(R)}$ for the random vector $\mathbf{X}$ using the expectation operation $E[.]$ as

$$\mathbf{R}_X^{(R)} = E[\mathbf{X}^*\mathbf{X}^{\mathrm{T}}] = \mathbf{W}^*E[\mathbf{V}^*\mathbf{V}^{\mathrm{T}}]\mathbf{W}^{\mathrm{T}}. \tag{10}$$

The correlation matrix of $\mathbf{V}$ (signal plus noise) is given by $S_V\mathbf{C}_{V_S}^{(R)} + N_V\mathbf{I}$, where $\mathbf{C}_{V_S}^{(R)}$ is given in (4); $\mathbf{I}$ is the L-by-L identity matrix; S_V is the signal power; and N_V is

the noise power. Then, substituting the expression above for the correlation matrix of $\mathbf{V}$ in (10), using (6), distributing the matrix product, and using (5),

$$\mathbf{R}_X^{(R)} = (\mathbf{H}^{-1})^*[S_V\mathbf{C}_{V_S}^{(R)} + N_V\mathbf{I}](\mathbf{H}^{-1})^{\mathrm{T}} = S_V\mathbf{I} + N_V(\mathbf{H}^{\mathrm{T}}\mathbf{H}^*)^{-1}. \quad (11)$$

It is thus evident that the range-time correlation of $\mathbf{X}$ is the sum of a signal ($\mathbf{R}_{X_S}^{(R)}$) and a noise ($\mathbf{R}_{X_N}^{(R)}$) component, where $\mathbf{R}_{X_S}^{(R)} = S_V\mathbf{I}$ and $\mathbf{R}_{X_N}^{(R)} = N_V(\mathbf{H}^{\mathrm{T}}\mathbf{H}^*)^{-1}$. By definition, $\mathbf{X}_S$ is white because its correlation is a diagonal matrix. Additionally, all components have identical power S_V because $\mathbf{R}_{X_S}^{(R)}$ is a scalar multiple of the identity matrix. On the other hand, the noise becomes colored, and its mean power after whitening can be computed by averaging the powers of the individual components of $\mathbf{X}_N$, which correspond to the diagonal elements of $\mathbf{R}_{X_N}^{(R)}$. Then,

$$N_X = \frac{1}{L}\,\mathrm{tr}[\mathbf{R}_{X_N}^{(R)}] = \frac{N_V}{L}\,\mathrm{tr}[(\mathbf{H}^{\mathrm{T}}\mathbf{H}^*)^{-1}], \quad (12)$$

where tr(.) is the matrix trace operation. Therefore, the noise enhancement factor (NEF) defined as NEF $= N_X/N_V$ can be obtained from (12) as

$$\mathrm{NEF} = L^{-1}\,\mathrm{tr}\{[\mathbf{C}_{V_S}^{(R)}]^{-1}\}, \quad (13)$$

where we used the cyclic property of the trace and the matrix decomposition in (5). For an ideal system (i.e., a system with a rectangular transmitted pulse and radar bandwidth much larger than the reciprocal of pulse width) $\rho_V^{(R)}(l) = 1 - |l|/L$ for $|l| < L$, and the trace in (13) can be computed using (A32) to obtain NEF $= L^2(L + 1)^{-1}$. Note that an extra L factor should be added if comparing with the noise power in the classical processing. To effectively oversample by a factor of L, an L-times larger bandwidth than the reciprocal of the pulse width is needed; this increases the noise power by the same factor. Under these considerations, the effective noise increase over the matched filter case (for an ideal system) becomes $L^3(L + 1)^{-1}$.

The trade-off between noise enhancement (radar sensitivity) and variance reduction makes the whitening transformation useful in cases of relatively large SNR. For weather surveillance radars, the SNR of signals from storms is large and the effects of noise when using the whitening transformation are negligible. For example, a 3 mm h^{-1} rain in the Weather Surveillance Radar-1988 Doppler (WSR-88D) produces an SNR of 37 dB at 50 km. Clearly, for measuring light rain, the noise enhancement by whitening would not be a problem to the full 230 km of required coverage. However, the threshold for display is set at an SNR of 6 dB mainly to observe snow, which typically has smaller reflectivity. This SNR falls in the range where noise enhancement dominates and may preclude the use of whitening.

A solution to the noise enhancement problem is to relax the whitening requirements and select a transformation such that the output noise power is also minimized. A transformation that is optimized based on the minimum mean-square error (MMSE) criterion accomplishes the desired goal but requires a priori knowledge of the SNR at every range location (Ebbini et al. 1993). Alternatively, we can look at the same problem in terms of the eigenvalues of the range-time correlation matrix. The ability to limit the gain of the whitening transformation to reduce the noise enhancement effect arises from the relation between the eigenvalues of a correlation matrix and the corresponding power spectral density. That is, the range spanned by the power spectral density matches closely the range of eigenvalues (Johnson and Dudgeon 1993). Accordingly, by limiting the span of eigenvalues, it is possible to place a bound on the gain of the transformation (Torres 2001). The analysis of these and other suboptimal techniques is a subject for further study.

5. Spectral moment estimators

The estimation of spectral moments using a whitening transformation on oversampled data is performed in three steps. First, oversampled data in range are whitened as discussed in section 3. Then, the sample-time autocorrelation at lags zero and one are estimated for each range location, and these estimates are averaged (in range) to reduce the standard errors. Finally, these improved correlation estimates are used to compute power, Doppler velocity, and Doppler spectrum width with the usual algorithms (Doviak and Zrnić 1993). Whitening-transformation-based (WTB) estimators for the spectral moments and the theoretically derived equations for their variances (appendix A) are presented next. These theoretical equations are used to compare and validate simulation results. Further, they clearly show the interplay of the various variables in the reduction of variances.

a. Signal power estimator

The WTB power estimator for oversampled signals in noise is given by

$$\underset{(\mathrm{WTB})}{\hat{S}} = \hat{S}_X = \frac{1}{LM}\sum_{l=0}^{L-1}\sum_{m=0}^{M-1}|X(l, m)|^2 - N(\mathrm{NEF}), \quad (14)$$

where L is the oversampling factor, M is the number of pulses, N is the noise power, NEF is the noise enhancement factor in (13), and $X(l, n)$ is the whitened oversampled weather signal as in (7). Using the results in the appendix for an ideal system, the normalized standard deviation of WTB signal power estimates is obtained from (A34) as

$$\frac{\mathrm{SD}\{\hat{S}\}}{\underset{(\mathrm{WTB})}{S}} = \frac{1}{\sqrt{M}}\left[\frac{1}{2\sigma_{\mathrm{vn}}\sqrt{\pi}}\frac{1}{L} + \frac{2L}{L+1}\left(\frac{N}{S}\right) + \frac{L(3L^2 + 2L - 3)}{2(L+1)^2}\left(\frac{N}{S}\right)^2\right]^{1/2}, \quad (15)$$

where σ_{vn}, the normalized spectrum width, is defined as $\sigma_v/2v_a$, and v_a is the maximum unambiguous velocity.

b. Mean Doppler velocity estimator

The WTB mean Doppler velocity estimator for oversampled signals is given by

$$\underset{(\mathrm{WTB})}{\hat{v}} = -\frac{v_a}{\pi}\arg[\hat{R}_X^{(T)}(1)], \tag{16}$$

where v_a is the maximum unambiguous velocity, and the lag-one sample-time autocorrelation function for the oversampled whitened signal $X(l, n)$ is estimated as

$$\hat{R}_X^{(T)}(1) = \frac{1}{L}\sum_{l=0}^{L-1}\hat{R}_{X_l}^{(T)}(1) = \frac{1}{L(M-1)}\sum_{l=0}^{L-1}\sum_{m=0}^{M-2}X^*(l, m)X(l, m+1), \tag{17}$$

where $X(l, n)$ is the whitened oversampled weather signal. From (A35) in the appendix, the standard deviation of WTB mean Doppler velocity estimates for the ideal case is

$$\frac{\mathrm{SD}\{\hat{v}\}_{(\mathrm{WTB})}}{2v_a} = \frac{1}{2\pi\sqrt{M-1}}\left\{\left[\frac{e^{(2\pi\sigma_{vn})^2}-1}{4\sigma_{vn}\sqrt{\pi}}\right]\frac{1}{L} + [2\sinh(2\pi\sigma_{vn})^2]\frac{L}{L+1}\left(\frac{N}{S}\right) + \left[\frac{e^{(2\pi\sigma_{vn})^2}}{2}\right]\frac{L(3L^2+2L-3)}{2(L+1)^2}\left(\frac{N}{S}\right)^2\right\}^{1/2}. \tag{18}$$

c. Doppler spectrum width estimator

The WTB Doppler spectrum width estimator for oversampled signals is given by

$$\underset{(\mathrm{WTB})}{\hat{\sigma}_v} = \frac{v_a\sqrt{2}}{\pi}\left|\ln\left[\frac{\hat{S}_X}{|\hat{R}_X^{(T)}(1)|}\right]\right|^{1/2}\mathrm{sgn}\left\{\ln\left[\frac{\hat{S}_X}{|\hat{R}_X^{(T)}(1)|}\right]\right\}, \tag{19}$$

where $\hat{S}_X$ and $\hat{R}_X^{(T)}(1)$ are given in (14) and (17), respectively. From (A36) in the appendix, the standard deviation of WTB Doppler spectrum width estimates for the ideal case is

$$\frac{\mathrm{SD}\{\hat{\sigma}_v\}_{(\mathrm{WTB})}}{2v_a} = \left[\frac{e^{(2\pi\sigma_{vn})^2}}{4\pi^2\sigma_{vn}}\right]\frac{1}{\sqrt{M-1}} \times \left\{\left[\frac{e^{(2\pi\sigma_{vn})^2}-4e^{(\pi\sigma_{vn})^2}+3}{4\sigma_{vn}\sqrt{\pi}}\right]\frac{1}{L} + 2[\cosh(2\pi\sigma_{vn})^2-1]\frac{L}{L+1}\left(\frac{N}{S}\right) + \left[\frac{e^{(2\pi\sigma_{vn})^2}+2}{2}\right]\frac{L(3L^2+2L-3)}{2(L+1)^2}\left(\frac{N}{S}\right)^2\right\}^{1/2}. \tag{20}$$

d. Results

The performance of WTB estimators is compared with that achieved by the classical matched-filter-based (MFB) estimators and the estimators obtained from oversampled data and regular averaging. MFB estimators are derived from oversampled data using coherent range averaging, that is, the type of conventional processing that uses a digital matched filter at the receiver's front end (averaging in range is performed at the I and Q component level). Alternatively, oversampling-and-average-based (OAB) estimators operate on oversampled data but use incoherent averaging; that is, averaging in range is performed at the correlation level. Throughout this work we stress the comparison of WTB estimates, (the proposed implementation) with MFB estimates, the current implementation in the WSR-88D. OAB estimators are only included for illustrative purposes; for more details the reader is referred to Torres (2001).

Figure 2 shows the normalized standard deviation of WTB, MFB, and OAB power (Fig. 2a), Doppler velocity (Fig. 2b), and spectrum width estimators (Fig. 2c) as a function of the SNR for the ideal case and a normalized spectrum width of 0.08. The oversampling factor $L = 8$ is a realistic value that can be achieved on weather surveillance radars. The SNR in these figures refers to the output of the digital receiver, before the digital matched filter for the case of MFB estimates. With this assumption one can make a fair comparison of estimates because the common signal path ends at the digital receiver. After the digital receiver, either whitening or a matched filter (or both) can be applied.

When compared with MFB (or OAB) estimates, WTB estimates exhibit a superior performance for large SNR. Nonetheless, it is evident from these plots that the performance of the WTB estimator worsens as the SNR decreases due to the noise-enhancement effect inherent to the whitening transformation. The performance of OAB estimators is not optimum in terms of variance reduction as the average is done on correlated variables. However, since there is no noise enhancement, OAB estimates exhibit lower errors than MFB estimates for a broader range of SNR than the WTB estimates. The variance reduction factor (VRF) for the three WTB estimators compared with the conventional matched-filter approach can be computed as the ratio of the variance of MFB estimates to the variance of WTB estimates.

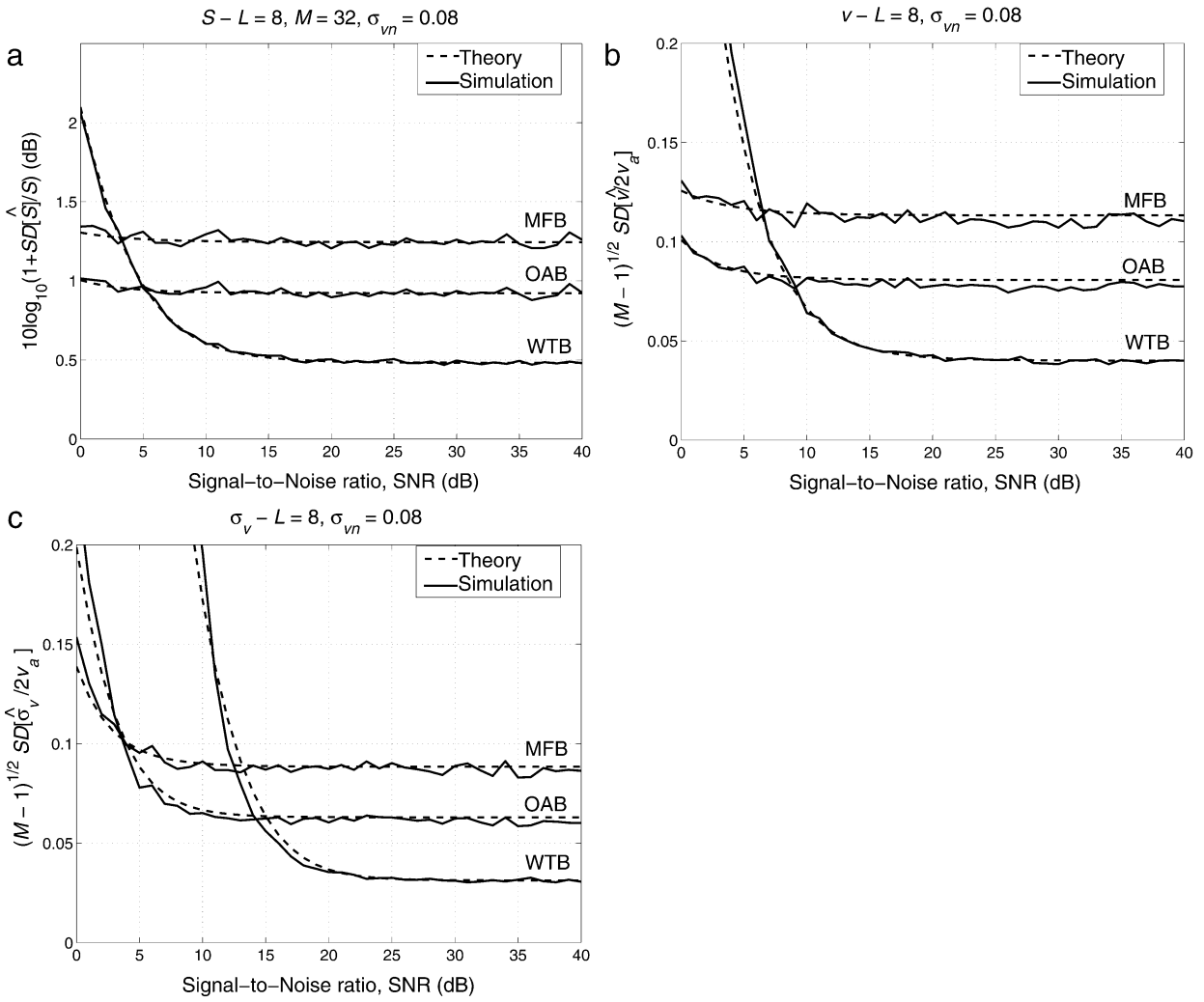

FIG. 2. Standard error of (a) signal power, (b) mean Doppler velocity, and (c) Doppler spectrum width estimates vs the SNR for the ideal case. The three sets of curves in each figure correspond to WTB, MFB, and OAB estimators, respectively. Solid lines show the results from simulations (averaging 1000 realizations), and dashed lines show the theoretical predictions.

For the ideal receiver case and a large SNR, the variance reduction factor is equal to the oversampling factor L [cf. (A34)–(A36) with (A39)–(A41), respectively]. Note that theoretical predictions and simulation results, both plotted in Fig. 2, are in remarkable agreement.

Figure 3 shows the bias of WTB, MFB, and OAB signal power (Fig. 3a), mean Doppler velocity (Fig. 3b), and spectrum width estimators (Fig. 3c) as a function of the SNR under the same conditions as in Fig. 2. Estimators of S and v are unbiased even for relatively low SNR. On the other hand, σ_v estimates exhibit a small bias even for large SNR with WTB estimates being the least biased of the three. At low SNR, WTB estimates of the spectrum width are heavily biased due to the noise-enhancement effect.

It is of practical significance to determine the value of SNR for which the variance of estimates obtained from whitened samples is equal to the variance of estimates in the matched-filter implementation. This is because WTB estimators should be utilized only for SNRs greater than or equal to the crossover signal-to-noise ratio (SNR_c). By definition, SNR_c is found by equating the VRF to 1 and is plotted in Fig. 4 versus the normalized spectrum width for power (Fig. 4a), Doppler velocity (Fig. 4b), and spectrum width estimates (Fig. 4c). For completeness, the SNR_c with respect to OAB estimates is also shown. These plots were obtained directly from the theoretical results derived in appendix A and verified by simulation studies (see appendix B).

6. Discussion

Section 5 discussed the application of the whitening transformation to the estimation of spectral moments. Estimators operating on whitened signals were termed

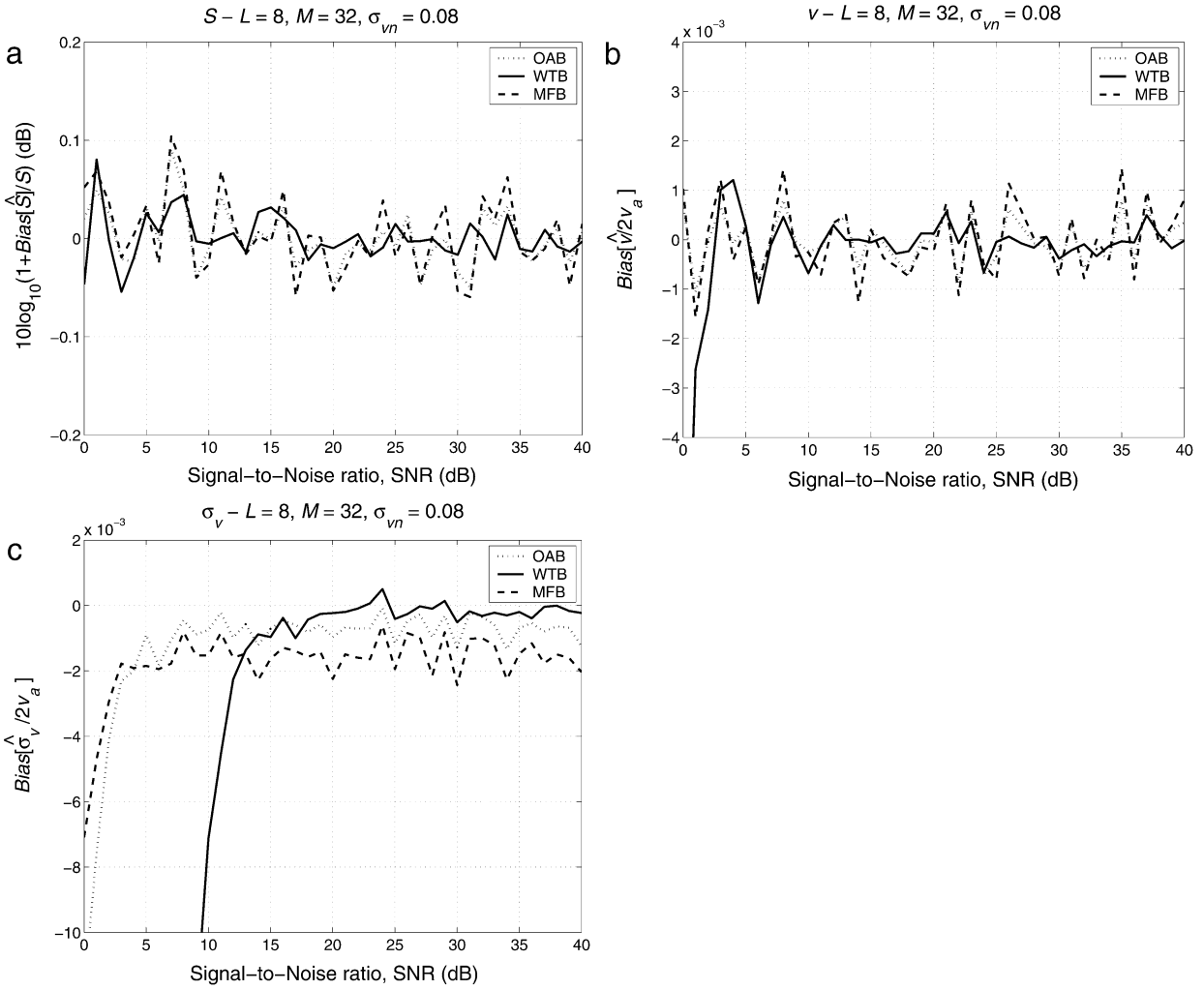

FIG. 3. Bias of (a) signal power, (b) mean Doppler velocity, and (c) Doppler spectrum width estimates vs the SNR for the ideal case. The three curves in each figure correspond to WTB, MFB, and OAB estimators, respectively. The results were obtained from simulations by averaging 1000 realizations.

WTB estimators, and they exhibit reduced standard errors with respect to MFB estimators if the SNR is relatively large. A performance comparison of all WTB estimators with MFB estimators for the ideal case showed that for all the variables the variance reduction factor for large SNR is L, where L is the oversampling factor. That is, approximately L-times fewer samples are needed for WTB estimators to keep the same errors as the ones obtained without the aid of a whitening transformation.

For low SNR, the performance of all WTB estimators deteriorates as the noise enhancement effect discussed in section 4 becomes significant. In such cases, the estimates on nonwhitened data result in better performance. The rule for selecting the best estimate is given by

$$\hat{\theta} = \begin{cases} \hat{\theta}_{(\mathrm{MFB})} & \text{if SNR} \le \mathrm{SNR}_c \\ \hat{\theta}_{(\mathrm{WTB})} & \text{if SNR} > \mathrm{SNR}_c. \end{cases} \tag{21}$$

In the previous equation, θ is any of the variables discussed in this chapter, namely, S, v, or σ_v; and SNR_c is the crossover SNR (different for each estimator) defined as the SNR that corresponds to a variance reduction factor of 1.

Throughout this study we dealt with an ideal system and a known range-time correlation coefficient, which derives from an assumption of uniform reflectivity. Although a rectangular pulse and infinite bandwidth receiver are not realistic, they closely approximate the characteristics of operational systems and serve to illustrate the potential of the method. For example, an intermediate-frequency (IF) bandwidth of about 10 times the reciprocal of the pulse width will be enough to still consider the noise white in relation with the weather signal bandwidth (what really counts is the value of the correlation coefficient of noise at lag 1, which we submit is close to zero in our application). This noise model differs from the one in Dias and Leitão (1993), where

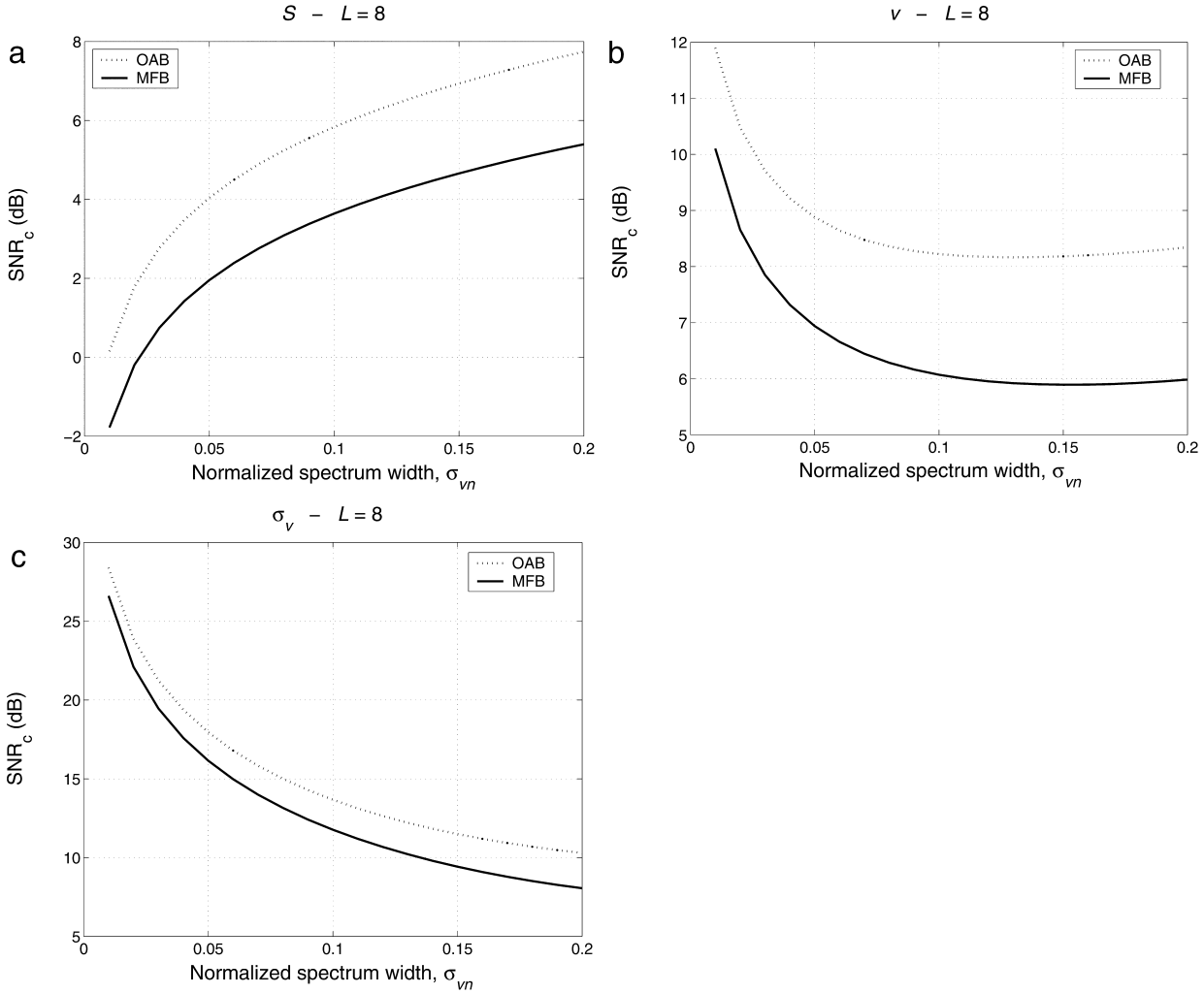

FIG. 4. SNR_c vs the normalized spectrum width for (a) signal power, (b) mean Doppler velocity, and (c) Doppler spectrum width estimators in an ideal system. Solid lines represent the SNR at which the errors of WTB estimates equal the errors of MFB estimates. Dashed lines represent the SNR at which the errors of WTB estimates equal the errors of OAB estimates. WTB estimates are accepted if SNR $>$ SNR_c; otherwise, classical estimates are preferred.

the assumption is that the noise and signal components are equally correlated in range and the noise is white only in sample time. In the National Weather Service (NWS) WSR-88D, the IF bandwidth exceeds 8 MHz and the short pulse is $\tau = 1.57$ μs; therefore, the bandwidth is over 12 times larger than the reciprocal of τ. In addition, although the transmitted pulse is not exactly rectangular, rise and fall times are short enough that experimental measurements of the range correlation of samples revealed an almost perfectly triangular correlation similar to the one assumed throughout this work.

The constraint of uniform reflectivity is the principal assumption required to precompute the exact correlation of oversampled signals in range. However, it is understood that these idealized conditions will not be satisfied for all the resolution volumes in an operational environment, especially at the edge of precipitation cells, where very sharp gradients could exist. Still, the assumption of uniform reflectivity has been used in practice before. For example, the WSR-88D averages four samples in range (over 1 km) to improve the accuracy of estimates. Thus, operational meteorologists ''accept'' averaging gradients over 1-km volume depths. Although the range extent of the resolution volume with the proposed method is smaller (about 500 m versus 1 km), degradation in regions of nonuniform reflectivity will occur, as shown through simulations by Torres (2001). For example, for a reflectivity gradient of 30 dB km^{-1} [referred to as ''extreme'' in model 1 of Rogers (1971)], it can be shown that the variance reduction factor is approximately cut in half. This is because the reflectivity profile modifies the correlation of range samples, and whitening based on uniformity assumptions is incomplete. However, the same simulation analyses showed that gradients of 10 dB km^{-1} would create negligible performance deterioration.

Approximate (or incomplete) whitening reduces the correlation of samples and hence the variance of estimates to a certain degree. Some decorrelation occurs regardless of reflectivity gradients because the range–time correlation function always has the same compact support; that is, it is zero outside of a finite interval that is solely dictated by the receiver impulse response and the transmitter pulse length. Implicit in the compactness is the assumption that the receiver bandwidth is much larger than the reciprocal of the pulse length. For example, for a finite-impulse-response (FIR) receiver filter with F taps, the support of the range-time correlation function is the symmetric interval of length $2(L + F)$ about zero, where L is the oversampling factor. Another way to look at this is in the frequency domain by examining the power spectral density of range samples. The support invariability of the correlation function implies that the nulls of the spectrum always correspond to the same frequencies. Since the whitening transformation is designed to boost those regions where the signal spectral components are weak, it follows that a considerable degree of whitening will be achieved even if there is a mismatch of correlation functions caused by reflectivity gradients. Further study with simulations as well as with real data is required to quantify this effect.

An alternative technique that increases the equivalent number of independent samples without the pitfalls of noise enhancement and correlation function mismatches is pulse compression. Then, it is natural to compare pulse compression to oversampling and whitening. Assume that peak transmitter power, pulse duration, and receiver bandwidth are the same for both techniques. In addition, the compressed pulses are averaged in range, and the number of averages is the same as the number of averages of whitened pulses in range. Then, at large SNRs, both achieve the same variance reduction of estimates because the oversampling factor (L) is equal to the compression factor. The difference is that pulse compression requires an L-fold increase in bandwidth for the transmitted signal. This increased bandwidth has a payoff at weak SNRs. If noise dominates estimation accuracy, pulse compression has approximately an L^2 edge in SNR over whitening. This is because there is an L-fold increase in signal power and, further, the noise is not enhanced by about a factor of L as occurs with whitening. In fact, averaging one L-compressed pulse is equivalent to a matched filter in terms of SNR. The increase in bandwidth (noise power) is compensated for by an increase in signal power, and averaging in range L pulse-compressed samples affects signal and noise in the same way. In summary, pulse compression outperforms whitening for low SNRs, but its practical implementation is only affordable in remote sensing devices that can allocate large transmission bandwidths.

7. Conclusions

A method for estimation of Doppler spectral moments on pulsed weather radars was presented. The scheme exploits the idea of whitening to obtain independent samples, such as in the works of Dias and Leitão (1993), Schulz and Kostinski (1997), Koivunen and Kostinski (1999), Frehlich (1999), and Fjørtoft and Lopes (2001). It operates on oversampled echoes in range, and the spectral moments are estimated by suitably combining weighted averages of these oversampled signals with usual processing of samples (spaced at pulse repetition time) at a fixed range location. As with the previous works, the whitening transformation is used in such a way that the equivalent number of independent samples equals the number of samples available for averaging and, consequently, the variance of the estimates decreases significantly.

Whitening-transformation-based (WTB) estimators of spectral moments were explored, and their performance was compared with that of classical estimators that use a digital matched filter. The variance reduction achieved by WTB estimators under ideal conditions asymptotically tends to L for large signal-to-noise ratios (SNRs). For low SNRs there is a crossover point (SNR_c) for the variances of WTB and classical estimators. Analytical expressions that allow the computation of SNR_c for any variable and different conditions were derived. For SNRs larger than the SNR_c, WTB estimates are preferred over classical estimates. Below the SNR_c, the noise enhancement effect dominates and classical estimates are favored.

The application of this technique is possible because

- the correlation of samples in range is known exactly if the resolution volume is uniformly filled with scatterers (although not optimum, estimate variance reduction is also possible in resolution volumes with reflectivity gradients);
- the receiver bandwidth is large compared with the reciprocal of the pulse length; and
- for most weather phenomena of interest, the SNR is relatively high (above the SNR_c), so the increase of noise power is not critical and the method works well.

Realistic simulations (see appendix B) were performed using known statistical properties of signals reflected by scatterers in fluids. The simulations also take the known properties of the probing pulse and receiver filter to reconstruct a composite signal from distributed scatterers illuminated by the pulse. This work confirms that WTB estimators are indeed viable candidates for future enhancements of the WSR-88D radar network.

Summarizing, the use of WTB estimators of spectral moments allows increasing the speed of volume coverage by weather radar so that hazardous features can be detected more timely. It also leads to better estimates of precipitation and wind fields.

Acknowledgments. The authors would like to thank Chris Curtis for constructive discussions concerning the overall structure of this paper and the derivations in appendix A. We appreciate references brought to our

attention by two anonymous reviewers. The Federal Aviation Administration provided support for part of this work through Interagency Agreement DTFA 03-01-X9007. Funding for this research was provided under NOAA-OU Cooperative Agreement NA17RJ1227.

APPENDIX A

Derivation of Estimator Variances

Estimators of the spectral moments $\hat{S}$, $\hat{v}$, and $\hat{\sigma}_v$ are obtained from estimates of total power $\hat{P}$ and the sample-time (T), lag-one autocorrelation function $\hat{R}^{(T)}$ (1) as

$$\hat{S} = \hat{P} - N, \tag{A1}$$

$$\hat{v} = -\frac{v_a}{\pi}\arg[\hat{R}^{(T)}(1)], \tag{A2}$$

$$\hat{\sigma}_v = \frac{v_a\sqrt{2}}{\pi}\left|\ln\left[\frac{\hat{S}}{|\hat{R}^{(T)}(1)|}\right]\right|^{1/2}\operatorname{sgn}\left\{\ln\left[\frac{\hat{S}}{|\hat{R}^{(T)}(1)|}\right]\right\}, \tag{A3}$$

where N is the system noise power and v_a is the maximum unambiguous velocity.

Consider first the case of WTB estimators. Estimates of power and lag-one autocorrelation are given by

$$\hat{P}_X = \frac{1}{LM}\sum_{l=0}^{L-1}\sum_{m=0}^{M-1} X^*(l, m)X(l, m), \tag{A4}$$

$$\hat{R}_X^{(T)}(1) = \frac{1}{L(M-1)}\sum_{l=0}^{L-1}\sum_{m=0}^{M-2} X^*(l, m)X(l, m+1), \tag{A5}$$

where L is the oversampling factor, M is the number of pulses, and $X(l, m)$ is the whitened signal as in (7).

Whereas the variance of $\hat{S}$ can be obtained by direct computation, if the distributions of (A4) and (A5) are smooth and narrow around their mean values, the variances for $\hat{v}$ and $\hat{\sigma}_v$ can be computed using perturbation analysis (Zrnić 1977). The results are summarized here:

$$\operatorname*{Var}_{(\mathrm{WTB})}\{\hat{S}\} = \operatorname{Var}\{\hat{P}_X\}, \tag{A6}$$

$$\operatorname*{Var}_{(\mathrm{WTB})}\{\hat{v}\} = \left(\frac{v_a}{\pi}\right)^2\frac{1}{2}\operatorname{Re}\left\{\operatorname{Var}\left[\frac{|\hat{R}_X^{(T)}(1)|}{|R^{(T)}(1)|}\right] - \operatorname{Var}\left[\frac{\hat{R}_X^{(T)}(1)}{R^{(T)}(1)}\right]\right\}, \tag{A7}$$

$$\begin{aligned}\operatorname*{Var}_{(\mathrm{WTB})}\{\hat{\sigma}_v\} &= \left[\frac{v_a^2|R^{(T)}(1)|}{\pi^2\sigma_v S}\right]^2 \\ &\quad\times\left\langle\operatorname{Var}\left(\frac{\hat{P}_X}{S}\right) + \frac{1}{2}\operatorname{Re}\left\{\operatorname{Var}\left[\frac{|\hat{R}_X^{(T)}(1)|}{|R^{(T)}(1)|}\right] + \operatorname{Var}\left[\frac{\hat{R}_X^{(T)}(1)}{R^{(T)}(1)}\right]\right\}\right. \\ &\quad\left. - 2\operatorname{Re}\left\{\operatorname{Cov}\left[\frac{\hat{P}_X}{S}, \frac{\hat{R}_X^{(T)}(1)}{R^{(T)}(1)}\right]\right\}\right\rangle.\end{aligned} \tag{A8}$$

To find these variances we must evaluate the following four expressions:

$$E\{\hat{P}_X^2\} = \frac{1}{L^2M^2}\sum_{l=0}^{L-1}\sum_{l'=0}^{L-1}\sum_{m=0}^{M-1}\sum_{m'=0}^{M-1} E[X^*(l, m)X(l, m)X^*(l', m')X(l', m')], \tag{A9}$$

$$E\{|\hat{R}_X^{(T)}(1)|^2\} = \frac{1}{L^2(M-1)^2}\sum_{l=0}^{L-1}\sum_{l'=0}^{L-1}\sum_{m=0}^{M-2}\sum_{m'=0}^{M-2} E[X^*(l, m)X(l, m+1)X^*(l', m'+1)X(l', m')], \tag{A10}$$

$$E\{[\hat{R}_X^{(T)}(1)]^2\} = \frac{1}{L^2(M-1)^2}\sum_{l=0}^{L-1}\sum_{l'=0}^{L-1}\sum_{m=0}^{M-2}\sum_{m'=0}^{M-2} E[X^*(l, m)X(l, m+1)X^*(l', m')X(l', m'+1)], \tag{A11}$$

$$E\{\hat{P}_X\hat{R}_X^{(T)}(1)\} = \frac{1}{L^2M(M-1)}\sum_{l=0}^{L-1}\sum_{l'=0}^{L-1}\sum_{m=0}^{M-1}\sum_{m'=0}^{M-2} E[X^*(l, m)X(l, m)X^*(l', m')X(l', m'+1)]. \tag{A12}$$

The expectation operations $E[.]$ inside these expressions can be simplified using the identity

$$\begin{aligned}E[X_1^*X_2X_3^*X_4] &= E[X_1^*X_2]E[X_3^*X_4] \\ &\quad + E[X_1^*X_4]E[X_3^*X_2],\end{aligned} \tag{A13}$$

which is valid for zero-mean, complex, Gaussian random variables (Reed 1962). After applying this identity to (A9)–(A12), each expectation can be expressed as the autocorrelation of X at particular lags; that is, $E[X^*(l, m)X(k, n)] = R_x(k-l, n-m)$. For example, for (A9) we have

$$\begin{aligned}E\{\hat{P}_X^2\} &= \frac{1}{L^2M^2}\sum_{l,l',m,m'}\{E[X^*(l, m)X(l, m)] \\ &\qquad\times E[X^*(l', m')X(l', m')] \\ &\qquad + E[X^*(l, m)X(l', m')] \\ &\qquad\times E[X^*(l', m')X(l, m)]\} \\ &= \frac{1}{L^2M^2}\sum_{l,l',m,m'}[R_X(0, 0)]^2 \\ &\quad + R_X(l'-l, m'-m)R_X(l-l', m-m'),\end{aligned} \tag{A14}$$

Quadruple summations can be simplified by letting $l'' = l' - l$, $m'' = m' - m$, and collecting terms so that

$$\sum_{l=0}^{L-1}\sum_{l'=0}^{L-1}\sum_{m=0}^{M-1}\sum_{m'=0}^{M-1} f(l'-l, m'-m) = \sum_{l''=-L+1}^{L-1}\sum_{m''=-M+1}^{M-1}(L-|l''|)(M-|m''|)f(l'', m''). \quad \text{(A15)}$$

Then,

$$E\{\hat{P}_X^2 - P^2\} = \frac{1}{L^2M^2}\sum_{l=-L+1}^{L-1}\sum_{m=-M+1}^{M-1} \times (L-|l|)(M-|m|)|R_X(l, m)|^2. \quad \text{(A16)}$$

Analogously, the three remaining expressions become

$$E\{|\hat{R}_X^{(T)}(1)|^2 - |R^{(T)}(1)|^2\} = \frac{1}{L^2(M-1)^2}\sum_{l=-L+1}^{L-1}\sum_{m=-M+2}^{M-2} \times (L-|l|)(M-|m|-1)|R_X(l, m)|^2, \quad \text{(A17)}$$

$$E\{[\hat{R}_X^{(T)}(1)]^2 - [R^{(T)}(1)]^2\} = \frac{1}{L^2(M-1)^2}\sum_{l=-L+1}^{L-1}\sum_{m=-M+2}^{M-2} \times (L-|l|)(M-|m|-1)R_X(l, m+1) \times R_X^*(l, m-1), \quad \text{(A18)}$$

$$E\{\hat{P}_X\hat{R}_X^{(T)}(1) - PR^{(T)}(1)\} = \frac{1}{L^2M(M-1)}\sum_{l=-L+1}^{L-1}\sum_{m=-M+2}^{M-2} \times (L-|l|)(M-|m|-1)R_X(l, m+1)R_X^*(l, m). \quad \text{(A19)}$$

Because $X(l, m)$ has uncorrelated signal and noise components, the autocorrelation function can be decomposed into a sum of the signal (S) and noise (N) autocorrelation functions, that is, $R_X = R_{X_S} + R_{X_N}$. Also, because we are dealing with precipitation particles and the width of the range-weighting function [(4.22) of Doviak and Zrnić 1993] is much smaller than the pulse repetition time, the time and space dimensions are approximately independent [see, e.g., section 5.5 of Bringi and Chandrasekar (2001)]. Therefore, two-dimensional autocorrelation functions are separable (see, e.g., Dias and Leitão 1993) as they can be decomposed into a product of one-dimensional sample-time (T) and range–time (R) autocorrelation functions:

$$R_X(l, m) = R_{X_S}^{(R)}(l)R_{X_S}^{(T)}(m) + R_{X_N}^{(R)}(l)R_{X_N}^{(T)}(m). \quad \text{(A20)}$$

Double summations can now be decoupled and (A16) becomes

$$\begin{aligned} E\{\hat{P}_X^2 - P^2\} &= \frac{1}{L^2M^2}\sum_{l=-L+1}^{L-1}(L-|l|)|R_{X_S}^{(R)}(l)|^2 \times \sum_{m=-M+1}^{M-1}(M-|m|)|R_{X_S}^{(T)}(m)|^2 \\ &\quad + \frac{2}{L^2M^2}\,\mathrm{Re}\left\{\sum_{l=-L+1}^{L-1}(L-|l|)R_{X_S}^{(R)}(l)[R_{X_N}^{(R)}(l)]^* \times \sum_{m=-M+1}^{M-1}(M-|m|)R_{X_S}^{(T)}(m)[R_{X_N}^{(T)}(m)]^*\right\} \\ &\quad + \frac{1}{L^2M^2}\sum_{l=-L+1}^{L-1}(L-|l|)|R_{X_N}^{(R)}(l)|^2 \times \sum_{m=-M+1}^{M-1}(M-|m|)|R_{X_N}^{(T)}(m)|^2. \end{aligned} \quad \text{(A21)}$$

Recall that the whitening transformation is applied to the samples along the range dimension [see (8)]; the sample–time correlation of weather signals, which carries the information needed to estimate the spectral moments, is preserved after whitening. Therefore, for a Gaussian sample-time correlation function and white noise $R_{X_S}^T(m) = S\exp[-2(\pi\sigma_{vn}m)^2 + j2\pi v_n m]$ and $R_{X_N}^T(m) = N\delta(m)$, where $v_n = v/2v_a$ and $\sigma_{vn} = \sigma_v/2v_a$, are the normalized velocity and spectrum width, respectively (Doviak and Zrnić 1993). Summations in (A21) involving these functions can be approximated as

$$\sum_{m=-M+1}^{M-1}(M-|m|)|R_{X_S}^{(T)}(m)|^2 \approx S^2\int_{-\infty}^{\infty}(M-|x|)e^{-(2\pi\sigma_{vn}x)^2}\,dx \approx \frac{MS^2}{2\pi^{1/2}\sigma_{vn}}, \quad \text{(A22)}$$

if $M\sigma_{vn} \gg 1$,

$$\sum_{m=-M+1}^{M-1}(M-|m|)R_{X_S}^{(T)}(m)[R_{X_N}^{(T)}(m)]^* = MSN, \quad \text{(A23)}$$

$$\sum_{m=-M+1}^{M-1}(M-|m|)|R_{X_N}^{(T)}(m)|^2 = MN^2. \quad \text{(A24)}$$

Closed-form solutions for the summations involving range-time correlations can be obtained if we work with correlation matrices instead of correlation functions. To make the conversion we can use the identity[1] $\sum_{l=-L+1}^{L-1}(L-|l|)R_1(l)R_2^*(l) = \mathrm{tr}\{\mathbf{C}_1\mathbf{C}_2\}$, where $\mathbf{C}_1$ and $\mathbf{C}_2$ are the correlation matrices corresponding to the correlation functions R_1 and R_2, respectively, and tr{.} is the matrix

[1] This can be proved by expressing the trace as the sum of diagonal elements of the matrix product, expanding the matrix product using the Hermitian and Toeplitz properties of complex correlation matrices, and finally performing a simple substitution of summation indexes.

trace operation. The relevant terms from (A21) are converted as

$$\sum_{l=-L+1}^{L-1} (L - |l|)|R_{X_S}^{(R)}(l)|^2 = \mathrm{tr}\{[\mathbf{C}_{X_S}^{(R)}]^2\}, \quad \text{(A25)}$$

$$\sum_{l=-L+1}^{L-1} (L - |l|)R_{X_S}^{(R)}(l)[R_{X_N}^{(R)}(l)]^* = \mathrm{tr}\{\mathbf{C}_{X_S}^{(R)}\mathbf{C}_{X_N}^{(R)}\}, \quad \text{(A26)}$$

$$\sum_{l=-L+1}^{L-1} (L - |l|)|R_{X_N}^{(R)}(l)|^2 = \mathrm{tr}\{[\mathbf{C}_{X_N}^{(R)}]^2\}. \quad \text{(A27)}$$

Correlation matrices for the signal and noise components of the whitened sequence X can be obtained from the correlation matrix of the range (correlated) samples V by recalling that $\mathbf{X} = \mathbf{WV}$ (8), where $\mathbf{W} = \mathbf{H}^{-1}$ and $\mathbf{C}_{V_S}^{(R)} = \mathbf{H}^*\mathbf{H}^{\mathrm{T}}$. Due to the linear relationship between $\mathbf{V}$ and $\mathbf{X}$, the correlation matrix of X can be written as $\mathbf{C}_X^{(R)} = \mathbf{W}^*\mathbf{C}_V^{(R)}\mathbf{W}^{\mathrm{T}}$. Decomposing $\mathbf{C}_V^{(R)}$ into its signal and noise components and distributing the matrix products,

$$\mathbf{C}_X^{(R)} = \mathbf{W}^*(S\mathbf{C}_{V_S}^{(R)} + N\mathbf{I})\mathbf{W}^{\mathrm{T}} = S\mathbf{I} + N(\mathbf{W}^*\mathbf{W}^{\mathrm{T}}); \quad \text{(A28)}$$

therefore, $\mathbf{C}_{X_S}^{(R)} = \mathbf{I}$ and $\mathbf{C}_{X_N}^{(R)} = \mathbf{W}^*\mathbf{W}^{\mathrm{T}}$. Finally, (A25)–(A27) can be written as

$$\mathrm{tr}\{[\mathbf{C}_{X_S}^{(R)}]^2\} = \mathrm{tr}\{\mathbf{I}^2\} = L, \quad \text{(A29)}$$

$$\mathrm{tr}\{\mathbf{C}_{X_S}^{(R)}\mathbf{C}_{X_N}^{(R)}\} = \mathrm{tr}\{\mathbf{W}^*\mathbf{W}^{\mathrm{T}}\} = \mathrm{tr}\{\mathbf{W}^{\mathrm{T}}\mathbf{W}^*\} = \mathrm{tr}\{[\mathbf{C}_{V_S}^{(R)}]^{-1}\}, \quad \text{(A30)}$$

$$\mathrm{tr}\{[\mathbf{C}_{X_N}^{(R)}]^2\} = \mathrm{tr}\{\mathbf{W}^*\mathbf{W}^{\mathrm{T}}\mathbf{W}^*\mathbf{W}^{\mathrm{T}}\} = \mathrm{tr}\{[\mathbf{C}_{V_S}^{(R)}]^{-2}\}. \quad \text{(A31)}$$

For the ideal range-time correlation coefficient (corresponding to a rectangular transmitter pulse and an infinite receiver bandwidth) the elements of the received signal correlation matrix are $(\mathbf{C}_{V_S}^{(R)})_{ij} = 1 - |j - i|L^{-1}$ $(1 \le i, j \le L)$. The structure of this matrix allows of computation of a closed-form expression for its inverse. It can be verified by matrix multiplication that

$$[\mathbf{C}_{V_S}^{(R)}]^{-1} = \begin{bmatrix} \frac{L(L+2)}{2L+2} & -\frac{L}{2} & 0 & \cdots & 0 & \frac{L}{2L+2} \\ -\frac{L}{2} & L & -\frac{L}{2} & \ddots & & 0 \\ 0 & -\frac{L}{2} & \ddots & \ddots & \ddots & \vdots \\ \vdots & \ddots & \ddots & \ddots & \ddots & 0 \\ 0 & & \ddots & \ddots & L & -\frac{L}{2} \\ \frac{L}{2L+2} & 0 & \cdots & 0 & -\frac{L}{2} & \frac{L(L+2)}{2L+2} \end{bmatrix}. \quad \text{(A32)}$$

Then, by summing the diagonal elements of (A32), $\mathrm{tr}\{[\mathbf{C}_{V_S}^{(R)}]^{-1}\} = L^3(L+1)^{-1}$. In addition, for symmetric matrices $\mathrm{tr}(A^2) = \sum_i \sum_j (A)_{ij}^2$ and from (A32) we find that $\mathrm{tr}\{[\mathbf{C}_{V_S}^{(R)}]^{-2}\} = (1/2)L^3(3L^2 + 2L - 3)(L+1)^{-2}$.

Introducing the results of (A22)–(A24) and (A29)–(A31) into (A21) for the ideal case,

$$E\{\hat{P}_X^2 - P^2\} = \frac{S^2}{2ML\sigma_{\mathrm{vn}}\sqrt{\pi}} + \frac{2SN}{M}\frac{L}{L+1} + \frac{N^2}{M}\frac{L(3L^2 + 2L - 3)}{2(L+1)^2}. \quad \text{(A33)}$$

In a similar way we can derive expressions for (A17)–(A19) to use in (A7) and (A8). Doing so we arrive at the following simplified expressions for the variances of WTB spectral moment estimators:

$$\underset{(\mathrm{WTB})}{\mathrm{Var}\{\hat{S}\}} = \frac{S^2}{M}\left[\frac{1}{2\sigma_{\mathrm{vn}}\sqrt{\pi}}\left(\frac{1}{L}\right) + 2\left(\frac{L}{L+1}\right)\left(\frac{N}{S}\right) + \frac{L(3L^2 + 2L - 3)}{2(L+1)^2}\left(\frac{N}{S}\right)^2\right], \quad \text{(A34)}$$

$$\underset{(\mathrm{WTB})}{\mathrm{Var}\{\hat{v}\}} = \frac{v_a^2}{\pi^2(M-1)}\left\{\frac{e^{(2\pi\sigma_{\mathrm{vn}})^2} - 1}{4\sigma_{\mathrm{vn}}\sqrt{\pi}}\left(\frac{1}{L}\right) + 2\sinh(2\pi\sigma_{\mathrm{vn}})^2\left(\frac{L}{L+1}\right)\left(\frac{N}{S}\right) + \frac{e^{(2\pi\sigma_{\mathrm{vn}})^2}}{2}\left[\frac{L(3L^2 + 2L - 3)}{2(L+1)^2}\right]\left(\frac{N}{S}\right)^2\right\}, \quad \text{(A35)}$$

$$\underset{(\mathrm{WTB})}{\mathrm{Var}\{\hat{\sigma}_v\}} = \frac{v_a^2 e^{2(2\pi\sigma_{\mathrm{vn}})^2}}{4\pi^4\sigma_{\mathrm{vn}}^2(M-1)}\left\{\frac{e^{(2\pi\sigma_{\mathrm{vn}})^2} - 4e^{(\pi\sigma_{\mathrm{vn}})^2} + 3}{4\sigma_{\mathrm{vn}}\sqrt{\pi}}\left(\frac{1}{L}\right) + 2[\cosh(2\pi\sigma_{\mathrm{vn}})^2 - 1]\left(\frac{L}{L+1}\right)\left(\frac{N}{S}\right) + \frac{e^{(2\pi\sigma_{\mathrm{vn}})^2} + 2}{2}\left[\frac{L(3L^2 + 2L - 3)}{2(L+1)^2}\right]\left(\frac{N}{S}\right)^2\right\}. \quad \text{(A36)}$$

We can repeat the same procedure for the case of a digital matched filter where the only difference from the previous case is in the way that the total power and lag-one autocorrelation function are estimated. In this case

$$\hat{P}_Y = \frac{1}{M}\sum_{m=0}^{M-1} |Y(m)|^2, \tag{A37}$$

$$\hat{R}_Y^{(T)}(1) = \frac{1}{M-1}\sum_{m=0}^{M-2} Y^*(m)Y(m+1), \tag{A38}$$

where $Y(m) = \kappa \sum_{l=0}^{L-1} V(l, m)$ is the output of the digital matched filter and $\kappa = [3(2L^2 + 1)^{-1}]^{1/2}$ is a normalization factor that preserves the power of the input signal under ideal conditions. Following the steps outlined in the previous case we obtain the variances of the estimators for the matched-filter case as

$$\underset{(\mathrm{MFB})}{\mathrm{Var}\{\hat{S}\}} = \frac{S^2}{M}\left[\frac{1}{2\sigma_{\mathrm{vn}}\sqrt{\pi}} + 2\left(\frac{3L}{2L^2+1}\right)\left(\frac{N}{S}\right) + \left(\frac{3L}{2L^2+1}\right)^2\left(\frac{N}{S}\right)^2\right], \tag{A39}$$

$$\underset{(\mathrm{MFB})}{\mathrm{Var}\{\hat{v}\}} = \frac{v_a^2}{\pi^2(M-1)}\left[\frac{e^{(2\pi\sigma_{\mathrm{vn}})^2}-1}{4\sigma_{\mathrm{vn}}\sqrt{\pi}} + 2\sinh(2\pi\sigma_{\mathrm{vn}})^2\left(\frac{3L}{2L^2+1}\right)\left(\frac{N}{S}\right) + \frac{e^{(2\pi\sigma_{\mathrm{vn}})^2}}{2}\left(\frac{3L}{2L^2+1}\right)^2\left(\frac{N}{S}\right)^2\right], \tag{A40}$$

$$\underset{(\mathrm{MFB})}{\mathrm{Var}\{\hat{\sigma}_v\}} = \frac{v_a^2 e^{2(2\pi\sigma_{\mathrm{vn}})^2}}{4\pi^4\sigma_{\mathrm{vn}}^2(M-1)}\left\{\frac{e^{(2\pi\sigma_{\mathrm{vn}})^2} - 4e^{(\pi\sigma_{\mathrm{vn}})^2} + 3}{4\sigma_{\mathrm{vn}}\sqrt{\pi}} + 2[\cosh(2\pi\sigma_{\mathrm{vn}})^2 - 1]\left(\frac{3L}{2L^2+1}\right)\left(\frac{N}{S}\right) + \frac{e^{(2\pi\sigma_{\mathrm{vn}})^2}+2}{2}\left(\frac{3L}{2L^2+1}\right)^2\left(\frac{N}{S}\right)^2\right\}. \tag{A41}$$

APPENDIX B

Simulation of Oversampled Weather Echoes

The simulation method uses known statistical properties of signals reflected by scatterers in fluids and is based on the well-known procedure for generating single-polarization time series by Zrnić (1975). Further, it takes into account the known properties of the probing pulse and receiver filter to reconstruct a composite signal from the distributed scatterers illuminated by the pulse; therefore, it is not difficult to modify the procedure to include reflectivity gradients and additive noise. The constructed time series exhibits the required autocorrelation in range and sample time. This procedure is justified by the fact that at the horizontal incidence common to weather surveillance radars, raindrops can be regarded as frozen scatterers since the time separation between echoes from overlapping range intervals is very small.

Signals received by a Doppler weather surveillance radar at any given time are due to the superposition of the waves backscattered by the hydrometeors that are present in the radar resolution volume. The range location r_s of the resolution volume with respect to the radar depends on the time delay between the transmitted pulse and the sampling time τ_s as given by $r_s = c\tau_s/2$, where c is the speed of light.

The simulation procedure starts with oversampling in range (along the range-time axis) so that there are L samples during the pulse duration τ. The contribution of scatterers within the resolution volume is distributed among L slabs, where each slab encompasses a large number of hydrometeors but is represented by its equivalent scattering center, which backscatters the complex (I, Q) voltage $s(l)$. This is reasonable because there are numerous scatterers in the resolution volume so that their contribution causes the voltage backscattered by each slab to be a Gaussian complex random variable. Note that implicit is the assumption that the slabs are large compared with the radar wavelength and there are many uniformly distributed scatterers in each slab. Thus, each element of the sequence $s(l)$ is an independent, identically distributed (IID) complex Gaussian random variable (RV) with zero mean and unit variance. It is assumed that the slab centers are separated in range by $c\tau/2L$ and that the weather signal is sampled at a rate L-times faster than the reciprocal of the pulse width, that is, $\tau_o = \tau/L$ s apart. Figure B1 shows a simplified scheme of the basic elements involved in the simulation procedure.

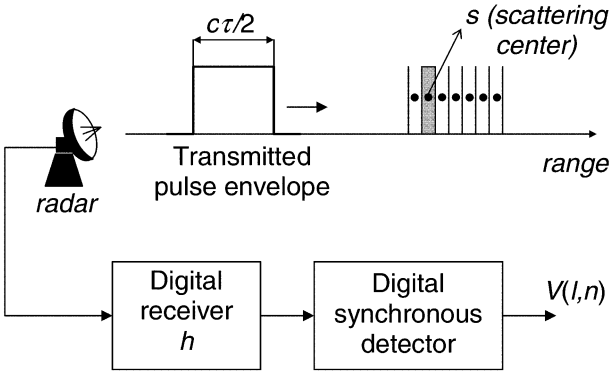

FIG. B1. Basic elements involved in the simulation of oversampled weather signals.

For an ideal (infinite bandwidth) receiver, the impulse response $h(n)$ is given by the unit-sample sequence, that is, $h(n) = \delta(n)$. If range time is indexed with l, a range sample of the weather signal is given by

$$V_1(l) = \sum_{i=0}^{L-1} s(l + i)p(L - 1 - i), \quad 0 \le l < L, \tag{B1}$$

where s is a $2L - 1$ vector of IID Gaussian random variables with zero mean and unit variance, and p is the transmitted pulse envelope. The autocorrelation of the signal in (B1) is

$$R_{V_1}^{(R)}(m) = \sum_{j=0}^{L-1} p(j)p(j - m), \tag{B2}$$

which agrees with (4.39) of Doviak and Zrnić (1993). A nonideal receiver channel can be modeled by assuming that the receiver is a linear, shift-invariant system with impulse response $h(n) \neq \delta(n)$. Then, the convolution operation $\star$ can be used to obtain

$$\begin{aligned} V_2(l) &= V_1(l) \star h(l) \\ &= \left[\sum_{i=0}^{L-1} s(l + i)p(L - 1 - i)\right] \star h(l). \end{aligned} \tag{B3}$$

The power of this signal is now affected by the receiver's filter. The mean signal power after adding correlation in range is $G = \sum_{l=0}^{F+L-2} |(h \star p)(l)|^2$, where F is the receiver's filter impulse response length. In addition, the length of the input data sequence V_1 in (B3) should be adjusted to $L + F - 1$ samples so that enough convolution samples are computed in order to bypass transients and obtain a sequence V_2 with L samples.

For Doppler measurements, the radar is pulsed at a sufficiently high rate so that the atmospheric phenomena produce correlated signal samples. Samples for every range location are taken at intervals of T_s s, giving origin to the ''sample time.'' It is generally assumed that the sample-time correlation of weather signals is Gaussian (Doviak and Zrnić 1993) and given by

$$\begin{aligned} R_V^{(T)}(m) &= E[V^*(l, n)V(l, n + m)] \\ &= S \exp[-8(\pi\sigma_v m T_s/\lambda)^2]e^{-j4\pi\overline{v}mT_s/\lambda}, \end{aligned} \tag{B4}$$

where the superscript (T) denotes sample time, λ is the radar wavelength, S is the weather signal mean power, $\overline{v}$ the mean Doppler velocity of scatterers, and σ_v the associated spectrum width. Observe that V in (B4) is a two-dimensional quantity where the first index corresponds to range time and the second one to sample time.

To incorporate the required correlation in sample time (B4), proceed as follows. Repeat the simulation in (B3) for M sample-time data points using independent realizations of s for each iteration. This generates a $(L + F - 1)$-by-M matrix V_3 given by

$$\begin{aligned} V_3(l, n) &= \left[\sum_{i=0}^{L-1} s(l + i, n)p(L - 1 - i)\right] \star h(l), \\ &\text{for } 0 \le l < L + F - 1 \quad \text{and} \\ &0 \le n < M, \end{aligned} \tag{B5}$$

where s is a $(2L + F - 2)$-by-M matrix of IID, zero-mean, unit-variance, Gaussian random variables. Transient removal can be accomplished by constructing a truncated version of V_3 as $V_4(l, n) = V_3(l + F - 1, n)$, for $0 \le l < L$ and $0 \le n < M$. It follows that for a given time (fixed n) the samples $V_4(l, n)$ for $0 \le l < L$ have a correlation given by (B2), and for a given range (fixed l) they are IID complex Gaussian RV with zero mean and variance G (see previous section). Therefore, the usual coloring procedure can be applied along sample time. Start by expressing the power spectrum (on a discrete Doppler velocity axis) of (B4) as

$$\begin{aligned} \varsigma(v_k) &= \frac{S}{\sqrt{2\pi}\sigma_v G} \exp\left[-\frac{(v_k - \overline{v})^2}{2\sigma_v^2}\right], \\ v_k &= -v_a + \frac{2kv_a}{M}, \\ &k = -M, -M + 1, \ldots, 2M - 1, \end{aligned} \tag{B6}$$

where v_a is the maximum unambiguous velocity. The next step is to alias this spectrum into the Nyquist interval (M samples) and then flip it to change the Doppler velocity axis to the frequency axis ($v = -\lambda f_d/2$). This ''flipped'' sequence is referred to as $\varsigma'(k)$, where $0 \le k < M$. Summarizing, the time series with sample–time correlation is obtained (for a fixed l) using discrete-time Fourier transforms ($\mathcal{F}$) as

$$\begin{aligned} V(l, n) &= \mathcal{F}^{-1}\{\mathcal{F}[V_4(l, n)]\sqrt{\varsigma'(k)}\}, \\ &0 \le l \le L - 1; \end{aligned} \tag{B7}$$

where V_4 is the truncated version of the time series with only range-time correlation, and V exhibits the required correlation in both range and sample time. Finally, note that because (B6) is normalized, the mean power of V is S, as required.

REFERENCES

Bamler, R., 1991: Doppler frequency estimation and the Cramer–Rao bound. *IEEE Trans. Geosci. Remote Sens.*, **29,** 385–390.

Bringi, V. N., and V. Chandrasekar, 2001: *Polarimetric Doppler Weather Radar: Principles and Applications.* Cambridge University Press, 636 pp.

Brunkow, D. A., 1999: A new receiver and signal processor for the CSU–Chill radar. Preprints, *29th Conf. on Radar Meteorology*, Montreal, QC, Canada, Amer. Meteor. Soc., 256–258.

Chornoboy, E. S., 1993: Optimal mean velocity estimation for Doppler weather radars. *IEEE Trans. Geosci. Remote Sens.*, **31,** 575–586.

Dias, J., and J. Leitão, 1993: Maximum likelihood estimation of spectral moments at low signal-to-noise ratios, *Proc. Int. Conf. on*

Acoustics, Speech, and Signal Processing, Minneapolis, MN, Institute of Electrical and Electronics Engineers, 149–152.

——, and ——, 2000: Nonparametric estimation of mean Doppler and spectral width. *IEEE Trans. Geosci. Remote Sens.*, **38,** 271–282.

Doviak, R. J., and D. S. Zrnić, 1993: *Doppler Radar and Weather Observations.* 2d ed. Academic Press, 562 pp.

Ebbini, E. S., P. C. Li, and J. Shen, 1993: A new SVD-based optimal inverse filter design for ultrasonic applications. *Proc. Ultrasonics Symp.*, Baltimore, MD, Institute of Electrical and Electronics Engineers, 1187–1190.

Faddeev, D. K., and V. N. Faddeeva, 1963: *Computational Methods of Linear Algebra.* W. H. Freeman and Co., 621 pp.

Fjørtoft, R., and A. Lopes, 2001: Estimation of the mean radar reflectivity from a finite number of correlated samples. *IEEE Trans. Geosci. Remote Sens.*, **39,** 196–199.

Frehlich, R., 1993: Cramer–Rao bound for Gaussian random processes and applications to radar processing of atmospheric signals. *IEEE Trans. Geosci. Remote Sens.*, **31,** 1123–1131.

——, 1999: Performance of maximum likelihood estimators of mean power and Doppler velocity with a priori knowledge of spectral width. *J. Atmos. Oceanic Technol.*, **16,** 1702–1709.

Ivić, I. R., 2001: Demonstration of an efficient method for estimating spectral moments. M.S. thesis, Dept. of Electrical and Computer Engineering, University of Oklahoma, 72 pp.

Johnson, D. H., and D. E. Dudgeon, 1993: *Array Signal Processing: Concepts and Techniques.* Prentice Hall, 533 pp.

Kay, S. M., 1993: *Fundamentals of Statistical Signal Processing: Estimation Theory.* Prentice Hall, 595 pp.

Koivunen, A. C., and A. B. Kostinski, 1999: The feasibility of data whitening to improve performance of weather radar. *J. Appl. Meteor.*, **38,** 741–749.

Kostinski, A. B., and A. C. Koivunen, 2000: On the condition number of Gaussian sample-covariance matrices. *IEEE Trans. Geosci. Remote Sens.*, **38,** 329–332.

Mudukutore, A. S., V. Chandrasekar, and R. J. Keeler, 1998: Pulse compression for weather radars. *IEEE Trans. Geosci. Remote Sens.*, **36,** 125–142.

Papoulis, A., 1984: *Probability, Random Variables, and Stochastic Processes.* 2d ed. McGraw-Hill, 576 pp.

Reed, I. S., 1962: On a moment theory for complex Gaussian processes. *IRE Trans. Inf. Theory*, **8,** 194–195.

Rogers, R. R., 1971: The effect of variable target reflectivity on weather radar measurements. *Quart. J. Roy. Meteor. Soc.*, **97,** 154–167.

Schulz, T. J., and A. B. Kostinski, 1997: Variance bounds on the estimation of reflectivity and polarization parameters in radar meteorology. *IEEE Trans. Geosci. Remote Sens.*, **35,** 248–255.

Strauch, R. G., and R. Frehlich, 1998: Doppler weather radar velocity measurement using a single pulse. *J. Atmos. Oceanic Technol.*, **15,** 804–808.

Therrien, C. W., 1992: *Discrete Random Signals and Statistical Signal Processing.* Prentice Hall, 727 pp.

Tong, L., 1995: Blind sequence estimation. *IEEE Trans. Commun.*, **43,** 2986–2994.

Torres, S., 2001: Estimation of Doppler and polarimetric variables for weather radars. Ph.D. dissertation, University of Oklahoma, 158 pp.

Urkowitz, H., and S. L. Katz, 1996: The relation between range sampling rate, system bandwidth, and variance reduction in spectral averaging for meteorological radar. *IEEE Trans. Geosci. Remote Sens.*, **34,** 612–618.

Walker, G. B., P. S. Ray, D. S. Zrnić, and R. J. Doviak, 1980: Time, angle, and range averaging of radar echoes from distributed targets. *J. Appl. Meteor.*, **19,** 315–323.

Zrnić, D. S., 1975: Simulation of weatherlike Doppler spectra and signals. *J. Appl. Meteor.*, **14,** 619–620.

——, 1977: Spectral moment estimates from correlated pulse pairs. *IEEE Trans. Aerosp. Electron. Syst.*, **13,** 344–354.

——, 1979: Estimation of spectral moments for weather echoes. *IEEE Trans. Geosci. Remote Sens.*, **17,** 113–128.